UNIVERSITÄT SALZBURG

FINGERPRINT RECOGNITION UNDER THE INFLUENCE OF IMAGE SENSOR AGEING

Christof Kauba Andreas Uhl

Technical Report 2015-10 October 2015

Department of Computer Sciences

Jakob-Haringer-Straße 2
5020 Salzburg
Austria
www.cosy.sbg.ac.at

Technical Report Series

FINGERPRINT RECOGNITION UNDER THE INFLUENCE OF IMAGE SENSOR AGEING

Christof Kauba and Andreas Uhl

Department of Computer Sciences, University of Salzburg
Jakob-Haringer-Str. 2, 5020 Salzburg, AUSTRIA
Email: {ckauba, uhl}@cosy.sbg.ac.at

ABSTRACT

Fingerprint recognition performance is affected by many factors. One of these are defective pixels caused by ageing effects of the image sensor. We investigate the impact of these image sensor ageing related pixel defects on the performance of different fingerprint matchers (NBIS, VeriFinger, FingerCode and Phase Only Correlation). The matchers are compared against each other to quantify the differences in the impact. In practice also other influences besides image sensor ageing related effects are present. As we aim to evaluate the impact of the defective pixels only, disregarding template ageing and other external influences, it is not possible to use real image data. Instead an experimental study using an ageing simulation algorithm including hot and stuck pixels is conducted on the FVC2002 and FVC2004 data sets.

Index Terms— Image sensor ageing, hot pixels, stuck pixels, template ageing, fingerprint recognition performance

1. INTRODUCTION

Fingerprint recognition systems are well established nowadays because of their advantages over password or token based authentication. Most fingerprint scanners are using an optical image sensor. The quality of a fingerprint image can be degraded by many factors, e.g. finger surface conditions, dirt on the sensor's surface, external noise and misplacement. Another type of distortion impacting the image quality are image sensor defects caused by ageing effects. This leads to isolated defective pixels, appearing as point like, spiky shot noise in the output images. Image sensor ageing and its impact on the output images belongs to image and video forensics.

Although there is some related work on finger vein and hand vein recognition systems [1, 2], to the best of our knowledge the impact of these pixel defects on the performance of fingerprint recognition systems has not yet been studied. The contribution of this work is to investigate the impact of sensor ageing related pixel defects on the recognition performance of different fingerprint matchers in terms of the EER (Equal Error Rate), the FMR1000 and ZeroFMR. Different types of feature extraction and matching schemes may react differently. Thus two minutiae-based matchers, one ridge feature based matcher and one correlation based matcher are evaluated. Actually this corresponds to investigating the robustness of these matchers against spiky shot noise.

At first, based on the technical data of a real fingerprint scanner, the DigitalPersona U.are.U 4000B, the defect growth rate is estimated using an empirical formula. Sensor ageing belongs to the template ageing effect in biometrics. Other reasons for template ageing are biological ageing of the subject, changes in subject behaviour and changes in the acquisition conditions. All these lead to a lower recognition performance. Our aim is to isolate the impact of image sensor ageing and to find out which role it plays in biometric template ageing. Using real world fingerprint images is not possible because there are always other effects in addition to image sensor ageing present like subject ageing and changes in environmental conditions, which further degrade the recognition performance. In order to be able to quantify the impact of image sensor ageing related pixel defects exclusively, we use an ageing simulation algorithm based on our simplified pixel model to create several sets of aged images. For the simulations and the subsequent evaluations the FVC2002 [3] and FVC2004 [4] fingerprint data sets are used. For the two minutiae-based matchers on the FVC2004 data set the evaluations are repeated with templates aged.

The rest of this paper is organized as follows: Section 2 gives a brief overview on image sensor ageing, presents the pixel defect model and explains the ageing simulation algorithm. Section 3 outlines the four fingerprint matchers. Section 4 describes the experimental setup and provides the results. Section 5 concludes this work.

2. IMAGE SENSOR AGEING

Most biometric sensors contain some kind of image sensor, especially optical fingerprint scanners. An image sensor is an analogue device, which basically consists of an array of photosensitive cells, called pixels. Like every human being and every electronic device also an image sensor ages. Ageing becomes noticeable in form of defective pixels, showing different characteristics than at manufacturing time, even if the sensor is not in use. They appear as spiky shot noise in the output image and thus degrade the image quality.

2.1. Mechanism Causing the Defects

Pixel defects are permanent, inter-defect times follow an exponential distribution, indicating a constant defect rate and they are randomly distributed over the sensor area. According to the literature [5] the main defect causing source is cosmic ray radiation, actually the neutrons of the cosmic rays. Leung et al. [6] applied statistical analysis to the spatial and temporal distribution of defects. They showed that the spatial distribution of defects across the sensor area follows a normal random distribution with no significant bias towards short or long distances, i.e. no defect clustering. They also showed that inter-defect times follow an exponential distribution, indicating a constant defect rate. Both is in contradiction to material degradation as defect source. We focus on in-field defects only. Manufacture time defects occur during the fabrication process and may also include stuck and abnormal sensitivity pixels but are usually corrected by factory calibration, i.e. simply masked out.

2.2. Defect Types

The most prominent defect types that are developed over a sensor's lifetime are hot and stuck pixels.

A **hot pixel** is a defect that has an illumination independent component, which increases linearly with exposure time. It appears as a bright spot with a fixed location in the output image. A partially-stuck hot pixel has an additional component (offset) that is independent from the illumination and exposure time.

The output of a **stuck pixel** is always the same arbitrary but fixed value c in the range $0 \leq c \leq 255$ (assuming an 8 bit image). Thus, its output is constant under all illuminations and exposure time independent. Stuck pixels mainly appear as factory time defects and Leung et al. [6] claim that they never found a true stuck pixel in field.

2.3. Pixel Defect Model

A pixel model describes either the raw output of a single pixel or the whole sensor considering the incoming illumination and the impact of pixel defects. For this work we adopted the pixel model of Bergmüller et al. [7], which is a simplified version of Jessica Fridrich's pixel model [8]. As we aim for reproducible tests, modelling noise and environmental influences should be minimised. In fact, they can be eliminated completely in a simulation. All images are taken with the same sensor using the same exposure settings, thus the exposure time is constant and the PRNU can be eliminated. The dark current level is usually low for short exposure times used for capturing fingerprint images. This yields the simplified pixel model (y is the output of a single pixel, i is the incident illumination):

$$y = i + d + c \;\; with \;\; y, i, c, d \in \mathbb{R} \tag{1}$$

If the dark current d of a pixel is extremely high, it is often denoted as hot pixel. Whereas if the offset c is high, this results in a saturated pixel and is sometimes denoted as stuck pixel. As the definitions in the literature are not consistent, we define the following pixel model for our experiments:

$$y = c \qquad y = i + d \tag{2}$$

where the first one is light independent and has a constant value c, denoted as stuck pixel. The second one adds an offset to the incident illumination and is referred as hot pixel. The pixel model for 8 bit grey-scale images is:

$$Y(x,y) = \begin{cases} C(x,y) & if\, C(x,y) \neq 0 \\ I(x,y) + D(x,y) & otherwise \end{cases} \tag{3}$$
$$with \;\; Y, C, I, D \in (\mathbb{Z} : [0; 255]^{w \times h})$$

where C and D are the defect matrices (same size as the image, storing the stuck pixel value or hot pixel offset value, respectively), I is the incident illumination and x and y are the pixel's coordinates. A pixel's output $Y(x, y)$ saturates at 0 and 255 if interval borders are exceeded. This pixel model is the basis for the ageing simulation algorithm.

2.4. Image Ageing Simulation Algorithm

Our aim is to investigate solely the role image sensor ageing related effects play within the biometric template ageing effect and thus its impact on the recognition performance, disregarding additional effects like capturing conditions and subject ageing. Therefore we simulate the pixel defects. Although some researchers [9, 6] never found a true stuck pixel, we include it in our simulations. We use the same simulation algorithm as in [1], which is an extended version of the original algorithm proposed by Bergmüller et al. [7]. The algorithm takes an (unaged) image sequence as input and outputs several aged versions of this image sequence. At first it calculates the defect matrices C and D according to the pixel model. These are then applied to the input images to generate the aged versions. Actually the incident illumination I should be used according to our pixel model. Since it is not known, the sensor ageing related hot and stuck pixels are directly added to the unaged images, i.e. an offset d is added to a pixel's value for hot pixels and its value is replaced by c for stuck pixels. C and D are calculated recursively to comply with the once defective - always defective principle.

2.5. Empiric Formula for Estimating Defect Growth Rate

Chapman et al. [9] derived an empirical formula for estimating the defect growth rate based on the sensor technology (CCD or APS) and on sensor design parameters like sensor area, pixel size and gain (adjusted by the ISO setting):

$$D = A \cdot S^B \cdot ISO^C \tag{4}$$

where D is the defect density (defects/year/mm²), A is the number of defects/year/mm² if the pixel size is 1µm, S is the pixel size, ISO is the ISO value according to the ISO setting of the image sensor and B and C are constants depending on the sensor type. For a CCD sensor $A = 0.0141$, $B = -2.25$ and $C = 0.69$ and for an APS sensor $A = 0.0742$, $B = -3.07$ and $C = 0.5$.

3. FINGERPRINT RECOGNITION

Different types of fingerprint recognition schemes react differently to image degradations. Therefore, we consider fundamentally different types of fingerprint feature extraction and matching schemes:

Correlation-Based Matcher: These approaches use the fingerprint images in their entirety, the global ridge and furrow (i.e. valley) structure of a fingerprint is decisive. Images are correlated at different rotational and translational alignments, image transform techniques may be utilised for that purpose. As a representative of this class, we use a custom implementation of the phase only correlation (POC) matcher [10].

Ridge Feature-Based Matcher: Matching algorithms in this category deal with the overall ridge and furrow structure in the fingerprint, yet in a localised manner. Characteristics like local ridge orientation or local ridge frequency are used to generate a set of appropriate features representing the individual fingerprint. As a representative of the ridge feature-based matcher type we use a custom implementation of the fingercode approach (FC) [11].

Minutiae-Based Matcher: The set of minutiae within each fingerprint is determined and stored as list, each minutia being represented (at least) by its location and direction. The matching process then basically tries to establish an optimal alignment between the minutiae sets of two fingerprints to be matched, resulting in a maximum number of pairings between minutiae from one set with compatible ones from the other set. As the first representative of the minutiae-based matcher type we use *mindtct* and *bozorth3* from the "NIST Biometric Image Software" (NBIS) package (available at `http://fingerprint.nist.gov/NBIS/`) for minutiae detection and matching, respectively. The second minutiae-based matcher type we use is *VeriFinger*, developed by *Neurotechnology* (available in form of the VeriFinger SDK 7.0 at `http://www.neurotechnology.com/verifinger.html`), denoted as VF. For more details on the SDK and the FC and POC approach the interested reader is referred to recent work [12].

4. EXPERIMENTS

The images of the FVC2002/FVC2004 DB1 and DB2 are used as ground truth during our evaluations. DB3 is not used because these images were captured using a thermal sensor and we only focus on optical image sensors. DB4 contains synthetically generated images and thus is not used either. FVC2004's test procedure to determine the EER, FMR1000 and ZeroFMR, is adopted. For details on the databases itself and the test protocol please refer to [4].

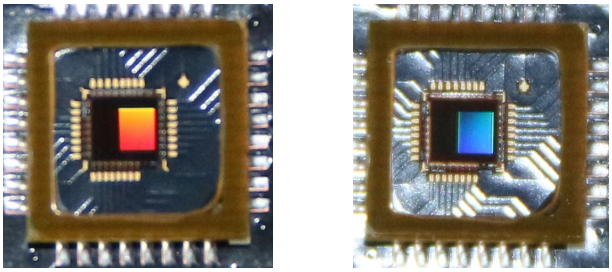

Fig. 1: Image sensor inside the U.are.U4000B fingerprint scanner

4.1. Experimental Settings

Bergmüller et al. [7] had two iris data sets available, captured with a time span of four years in between. They estimated the relative growth in the number of defective pixels, resulting in a defect rate of $0.6659\ defects/MP/year$. We have no two fingerprint data sets with a time lapse in between, taken with the same sensor. Thus, we use the formula of Chapman et al. [9] to estimate the defect growth rate based on the sensor data. There is no data concerning the image sensor used in the U.are.U 4000B fingerprint scanner available, thus we disassembled the device and measured the sensor area (see figure 1). The outside dimensions (dark yellow square) are $10.6 \times 10.6\,mm$ or about $410 \times 410\,pixels$ in the image. The actual image sensor area (red to yellow rectangle in the left and blue rectangle in the right picture) is about $77 \times 66 pixels$. This means that the sensor's dimensions are $1.99 \times 1.71\ mm$ which corresponds to a sensor area of $3.404\ mm^2$.

The images captured by the U.are.U 4000B and the U.are.U 4500 have a resolution of 356×328 pixels. Based on the measured sensor size of $3.404\ mm^2$ the pixel size is: $\frac{1.99}{356} \times \frac{1.71}{328} = 5.59 \times 5.21\ \mu m$. We assume a quadratic pixel size of $5.4\ \mu m$. Moreover there is no information available at which ISO level the FVC2002/FVC2004 images were captured, therefore we assume ISO level 400. Based on these specifications we get a defect rate of:

$$D = 3.404 \cdot 0.0742 \cdot 5.4^{-3.07} \cdot 400^{0.5} = \\ 0.0285\,defects/year = 0.244\,defects/MP/year \quad (5)$$

According to Chapman et al. [9] and Theuwissen [5] the additional offset of hot pixels or the dark current value, respectively, follows an exponential distribution, i.e. lower values are more likely to occur. The exponential distribution's parameter $\mu = 0.15$ was estimated based on their data.

In practice only very few defective pixels occur under normal conditions. At first we started the simulation with a defect rate of $1\ defect/MP/year$. In conditions with higher radiation like high altitudes or if electrical stress is imposed to the

sensor, the defect rates can become much higher. To account for such scenarios where higher defect rates might occur and as such a low number of defects had no impact on the recognition accuracy, we then decided to run our simulations with a rate of $4000\ defects/MP/year$, a time span of 10 years and time steps of 1 year.

We run the simulations for hot pixels only, stuck pixels only and combined stuck and hot pixels. To mitigate statistical fluctuations due to the random locations and amplitudes of the hot and stuck pixels, all tests were run 5 times (except for FC and POC due to time constraints) and the mean of the EER/ZeroFMR/FMR1000 is the final result. Only the probe images were aged but some of the experiments were conducted with aged template images (using the same pixel defects as the probe images), denoted as *TA*. An application scenario where not only the probe but also the template image are aged is establishing a biometric database using an old sensor which already suffers from ageing effects.

4.2. Experimental Results

Table 1 shows the EER, FMR1000 and ZeroFMR results for FVC2004 DB1. First of all the baseline values are given, followed by the values at a defect density of 40000 hot pixels per MP, 40000 stuck pixels per MP and 40000 combined hot and stuck pixels per MP. In addition a linear trend line is fitted to the EER data. The slope of this straight line is given as ***EER Slope*** in the table. The slope values given have to be multiplied by 10^{-8}, e.g. a value of 0.5 means $0.5 \cdot 10^{-8} = 5 \cdot 10^{-9}$. According to the baseline EER, FMR1000 and ZeroFMR values, VF is by far the best performing matcher, followed by FC, closely followed by NBIS. The worst performing matcher is POC. Figure 2 shows the EER for combined hot and stuck pixels. It can be seen that the ranking of the matchers does not change across the whole tested range. Looking at the increases in EER and their slopes, VF is influenced least, followed by POC and FC. NBIS is influenced most. This is in agreement with the FMR1000 and ZeroFMR values. FC shows a negative EER slope which indicates that its performance increases with an increasing number of defective pixels. In general the matching performance drops with an increasing defect rate but the highest increase in EER is only about 15%.

The results for FVC2004 DB2 are shown in Table 2 and Figure 3. Again on the unaged images VF performs best, followed by NBIS, then FC and POC performing worst. On DB2 both minutiae based matchers perform better than the correlation- and the ridge feature-based one. VF again performs best across the whole range tested and FC performs worst. No general decision if POC or NBIS performs better can be made. On DB2 VF is influenced least by all of the tested defect types. POC is influenced more than VF but not as much as NBIS and FC is influenced most. In general on DB2 hot pixels cause the least decrease in recognition performance, followed by hot and stuck pixels combined and stuck pixels lead to the highest decrease.On DB1, hot and stuck pixels combined lead to the most severe effects.

EER / Matcher	FC	POC	NBIS	NBIS *TA*	VF	VF *TA*
Base EER	0.126	0.216	0.136	0.136	0.025	0.025
Base FMR1000	0.703	0.637	0.359	0.359	0.056	0.056
Base ZeroFMR	0.728	0.686	0.473	0.473	0.086	0.086
Hot EER	0.125	0.223	0.15	0.152	0.027	0.027
EER Slope	-2.55	24	45.4	40.8	1.52	4.52
Hot FMR1000	0.669	0.634	0.364	0.366	0.057	0.056
Hot ZeroFMR	0.721	0.673	0.491	0.515	0.09	0.091
Stuck EER	0.13	0.204	0.156	0.153	0.027	0.029
EER Slope	-37.3	4.87	40.4	30.8	6.09	8.51
Stuck FMR1000	0.648	0.669	0.438	0.442	0.064	0.067
Stuck ZeroFMR	0.776	0.735	0.599	0.549	0.098	0.105
H+S EER	0.137	0.199	0.157	0.155	0.025	0.027
EER Slope	-15.3	5.27	22.7	17.2	2.63	7.18
H+S FMR1000	0.659	0.644	0.422	0.426	0.059	0.062
H+S ZeroFMR	0.831	0.697	0.582	0.537	0.096	0.097

Table 1: FVC2004 DB1 EER/FMR1000/ZeroFMR Summary

EER / Matcher	FC	POC	NBIS	NBIS *TA*	VF	VF *TA*
Base EER	0.101	0.104	0.093	0.093	0.025	0.025
Base FMR1000	0.358	0.363	0.266	0.266	0.044	0.044
Base ZeroFMR	0.471	0.565	0.358	0.358	0.053	0.053
Hot EER	0.103	0.104	0.099	0.109	0.025	0.027
EER Slope	8.48	6.3	21.8	44.1	-2.48	3.21
Hot FMR1000	0.36	0.299	0.288	0.295	0.043	0.045
Hot ZeroFMR	0.438	0.595	0.369	0.35	0.055	0.051
Stuck EER	0.177	0.116	0.119	0.133	0.029	0.03
EER Slope	162	40.5	70.5	112	6.43	13.2
Stuck FMR1000	0.445	0.373	0.351	0.397	0.046	0.055
Stuck ZeroFMR	0.518	0.556	0.431	0.459	0.057	0.071
Hot+Stuck EER	0.155	0.111	0.109	0.119	0.027	0.028
EER Slope	82	27.2	42.5	51.3	7.12	8.13
H+S FMR1000	0.418	0.345	0.307	0.315	0.046	0.051
H+S ZeroFMR	0.466	0.702	0.416	0.37	0.059	0.064

Table 2: FVC2004 DB2 EER/FMR1000/ZeroFMR Summary

Comparing Table 1 and Table 2 shows that the influence of pixel defects on DB2 is higher than on DB1 in general. Comparing DB1 and DB2 images shows that the absolute area in pixels covered by the fingerprint in DB1 images is larger than in DB2 images. Consequently the ridges and valleys are wider and thus less affected by single pixel defects. Hot pixels have less influence on DB1 than on DB2. This is also quite obvious as the background in the DB1 images is all white. A hot pixel simply adds an offset to the pixel value and if the pixel is already white, it stays white, i.e. no change. Moreover also stuck pixels have less influence on DB1. This is due to the higher contrast in general compared to DB2 images, i.e. the ridge lines appear darker and combined with the bright background this mitigates the influence of the single pixel defects.

Figure 4 shows the comparison between only probe images aged and probe and template images aged for the two minutiae based matchers on DB2. Looking at VF there is no clear trend if VF *TA* or VF performs better. On DB1 also NBIS *TA* and NBIS perform equally for hot pixels. However for stuck and combined hot+stuck pixels NBIS *TA* performs better than NBIS which is in a way the expected behaviour. If the templates are aged, the images will be more similar

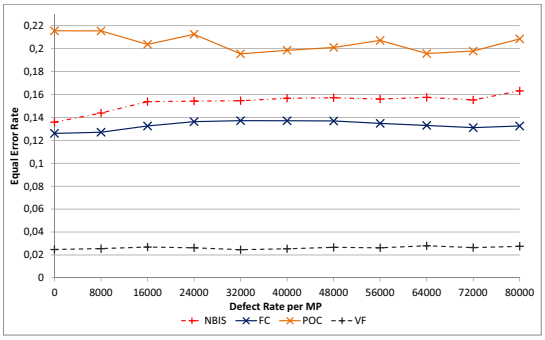

Fig. 2: FVC2004 DB1 EER Hot and Stuck Pixels

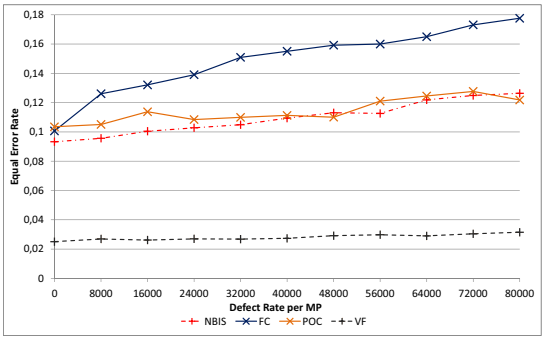

Fig. 3: FVC2004 DB2 EER Hot and Stuck Pixels

again and this should lead to improved matching results. On DB2 the situation is completely different. NBIS clearly outperforms NBIS *TA* with increasing defect density. Again the images start to look more similar which this time leads to an increase in the FMR and results in an increased EER.

The results for FVC2002 DB1 are shown in table 3, which has the same structure as table 1 for the FVC2004 results. Looking at the baseline values, it can be seen that VF again clearly performs best, followed by NBIS and then by FC. POC performs worst. The values in the table and also in figure 5 show that VF is influenced least by defective pixels, followed by NBIS and FC and POC is influenced most. VF has consistently low EER slope values, indicating that its EER remains almost constant even up to 40000 defects/MP. The influence on NBIS is also rather low. The two non-minutiae based matchers are influenced more but for a realistic number of defective pixels there is no significant drop in their performance. Again hot pixels have the least influence, followed by hot and stuck pixels combined and stuck pixels have the highest influence. In contrast to the other matchers, VF is influenced more by hot pixels than by stuck ones.

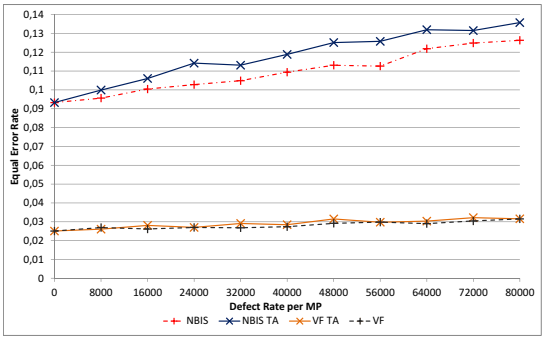

Fig. 4: FVC2004 DB2 EER NBIS + VF, Hot + Stuck Pixels

EER / Matcher	FC	POC	NBIS	VF
Baseline EER	0.133	0.164	0.034	0.006
Baseline FMR1000	0.538	0.455	0.086	0.01
Baseline ZeroFMR	0.661	0.623	0.113	0.008
40000 Hot EER	0.137	0.168	0.034	0.007
EER Slope	10.6	6.38	0.937	1.64
40000 Hot FMR1000	0.546	0.454	0.085	0.009
40000 Hot ZeroFMR	0.673	0.606	0.123	0.011
40000 Stuck EER	0.137	0.182	0.04	0.006
EER Slope	11.6	39.6	14	0.621
40000 Stuck FMR1000	0.603	0.448	0.103	0.008
40000 Stuck ZeroFMR	0.711	0.564	0.149	0.01
40000 Hot+Stuck EER	0.134	0.167	0.039	0.007
EER Slope	3.46	17	9.97	-0.767
40000 Hot+Stuck FMR1000	0.562	0.501	0.102	0.008
40000 Hot+Stuck ZeroFMR	0.722	0.593	0.127	0.01

Table 3: FVC2002 DB1 EER/FMR1000/ZeroFMR Summary

EER / Matcher	FC	POC	NBIS	VF
Baseline EER	0.108	0.162	0.026	0.007
Baseline FMR1000	0.267	0.401	0.051	0.007
Baseline ZeroFMR	0.29	0.525	0.069	0.007
40000 Hot EER	0.107	0.168	0.027	0.006
EER Slope	0.373	15.1	0.566	-1.29
40000 Hot FMR1000	0.259	0.399	0.058	0.007
40000 Hot ZeroFMR	0.287	0.559	0.085	0.007
40000 Stuck EER	0.119	0.178	0.03	0.005
EER Slope	29.6	40	11.8	-2.74
40000 Stuck FMR1000	0.296	0.439	0.061	0.006
40000 Stuck ZeroFMR	0.366	0.55	0.072	0.007
40000 Hot+Stuck EER	0.111	0.171	0.026	0.005
EER Slope	13.5	13.9	4.85	-4.46
40000 Hot+Stuck FMR1000	0.27	0.454	0.067	0.006
40000 Hot+Stuck ZeroFMR	0.349	0.557	0.081	0.007

Table 4: FVC2002 DB2 EER/FMR1000/ZeroFMR Summary

Table 4 and figure 6 show the results on FVC2002 DB2. Similar to DB1, VF clearly outperforms all other matchers. NBIS is ranked second, followed by FC and POC again performs worst. The performance of VF even increases with an increasing number of defects. Again the two minutiae based matchers are influenced less than FC and POC. VF and NBIS are not influenced at all for a reasonable number of defective pixels and the influence on FC and POC is negligible as well. By comparing the FVC2002 and FVC2004 results it can be seen that the minutiae-based matchers not only perform better than the non minutiae-based ones for high quality fingerprints but they are also less influenced by defective pixels for high quality fingerprints. The influence of image sensor ageing related pixel defects is lower if the baseline performance is higher, i.e. fingerprint images have higher quality.

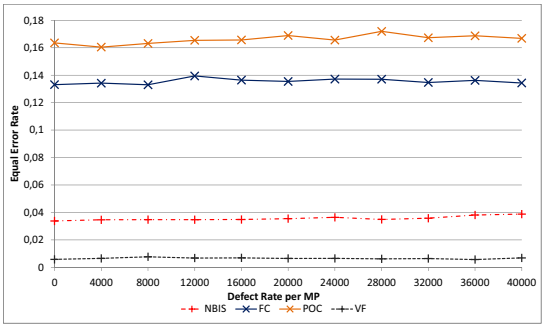

Fig. 5: FVC2002 DB1 EER Hot and Stuck Pixels

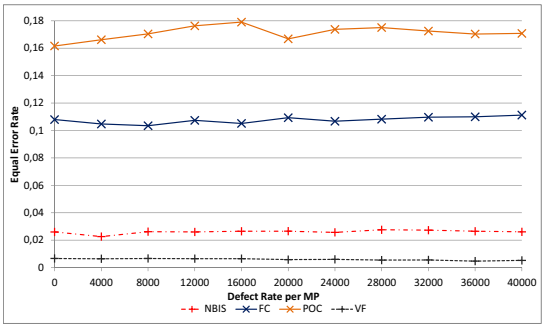

Fig. 6: FVC2002 DB2 EER Hot and Stuck Pixels

5. CONCLUSION

We investigated the influence of image sensor ageing related pixel defects within the biometric template ageing phenomenon on fingerprint recognition systems. We estimated the defect growth rate based on real sensor characteristics. On the one hand this estimated rate is quite low and does not lead to any influence on the recognition accuracy. On the other hand the model of Chapman et al. and Jessica Fridrich are only theoretical and not able to cover all the effects occuring inside a sensor in real-world applications leading not only to higher defect growth rates but also other effects having a negative imact on the image quality. To account for these other external influences and higher growth rates we used a much higher defect rate during our experiments.

Although there is a noticeable drop in the recognition performance for the unrealistic number of 20000 pixel defects per MP, most matchers are quite stable. Higher defect rates then $0.0285\,defects/year$ are likely to occur in practice because other external influences are present, but this would still only lead to a few defective pixels over a reasonable long sensor lifetime of 10 years. We showed that less than 1000 defects per MP have no impact on the recognition accuracy. In addition simple image denoising techniques were able to reduce the effect of defective pixels for finger and hand veins so the same should be true for fingerprints. Thus the contribution of defective pixels caused by image sensor ageing to the template ageing effect in fingerprinting is neglibile.

In conclusion defective pixels caused by image sensor ageing do not seem to be a problem in practical applications of fingerprint recognition.

6. REFERENCES

[1] Christof Kauba and Andreas Uhl, "Sensor ageing impact on finger-vein recognition," in *Proceedings of the 8th IAPR/IEEE International Conference on Biometrics (ICB'15)*, Phuket, Thailand, May 2015, pp. 1–8.

[2] Christof Kauba and Andreas Uhl, "Robustness evaluation of hand vein recognition systems," in *Proceedings of the International Conference of the Biometrics Special Interest Group (BIOSIG'15)*, Darmstadt, Germany, 2015, p. 8, accepted.

[3] Dario Maio, Davide Maltoni, Raffaele Cappelli, James L Wayman, and Anil K Jain, "Fvc2002: Second fingerprint verification competition," in *Pattern recognition, 2002. Proceedings. 16th international conference on*. IEEE, 2002, vol. 3, pp. 811–814.

[4] Dario Maio, Davide Maltoni, Raffaele Cappelli, Jim L Wayman, and Anil Jain, "Fvc2004: Third fingerprint verification competition," in *Biometric Authentication*, pp. 1–7. Springer, 2004.

[5] Albert JP Theuwissen, "Influence of terrestrial cosmic rays on the reliability of ccd image sensors-part 1: Experiments at room temperature," *Electron Devices, IEEE Transactions on*, vol. 54, no. 12, pp. 3260–3266, 2007.

[6] Jenny Leung, Jozsef Dudas, Glenn H Chapman, Israel Koren, and Zahava Koren, "Quantitative analysis of in-field defects in image sensor arrays," in *Defect and Fault-Tolerance in VLSI Systems, 2007. DFT'07. 22nd IEEE International Symposium on*. IEEE, 2007, pp. 526–534.

[7] Thomas Bergmüller, Luca Debiasi, Andreas Uhl, and Zhenan Sun, "Impact of sensor ageing on iris recognition," in *Proceedings of the IAPR/IEEE International Joint Conference on Biometrics (IJCB'14)*, 2014.

[8] Jessica Fridrich, "Sensor defects in digital image forensic," in *Digital Image Forensics*, pp. 179–218. Springer, 2013.

[9] Glenn H Chapman, Rohit Thomas, Zahava Koren, and Israel Koren, "Empirical formula for rates of hot pixel defects based on pixel size, sensor area, and iso," in *IS&T/SPIE Electronic Imaging*. International Society for Optics and Photonics, 2013, pp. 86590C–86590C.

[10] Hiroshi NAKAJIMA, Koji KOBAYASHI, and Tatsuo HIGUCHI, "A fingerprint matching algorithm using phase-only correlation," *IEICE Transactions on Fundamentals of Electronics, Communications and Computer Sciences*, vol. 87, no. 3, pp. 682–691, 2004.

[11] Anil K Jain, Salil Prabhakar, Lin Hong, and Sharath Pankanti, "Filterbank-based fingerprint matching," *Image Processing, IEEE Transactions on*, vol. 9, no. 5, pp. 846–859, 2000.

[12] Jutta Hämmerle-Uhl, Michael Pober, and Andreas Uhl, "Towards standardised fingerprint matching robustness assessment: the stirmark toolkit–cross-database comparisons with minutiae-based matching," in *Proceedings of the first ACM workshop on Information hiding and multimedia security*. ACM, 2013, pp. 111–116.